SUPPORTING INFORMATION

^{1}H NMR study of the influence of hemin vinyl→methyl substitution on the interaction between the C-terminus and substrate and the "aging" of the heme oxygenase from *Neisseria meningitidis*. Induction of active site structural heterogeneity by a two-fold symmetric hemin

Yangzhong Liu[#], *Li-Hua Ma*[#], *Xuhong Zhang*[‡], *Tadashi Yoshida*[‡], *James D. Satterlee*[§],

and Gerd N. La Mar[#*]

[#]Department of Chemistry, University of California, Davis, CA 95616; [‡]Department of Biochemistry, Yamagata University School of Medicine, Yamagata 990-9585, Japan and [§]Department of Chemistry, University of Washington, Pullman, WA 99164

Seven figures (Mass spectra for *Nm*HO^{A,X}-DMDH-CN complexes, NMR of CN^{-1} titration of *Nm*HO^{A,X}-DMDH-H_2O, NOESY spectra for inter-DMDH and peptide backbone contacts and upfield TOCSY spectra for *Nm*HO^{A}-DMDH-CN, NOESY spectra of NH contacts for *Nm*HO^{X}-DMDH-CN, and plots of δ_{dip}(obs) vs δ_{dip}(calc) for magnetic axis for *Nm*HO^{A}-PH-CN and *Nm*HO^{A}-DMDH-CN) and one table (Chemical shifts of assigned residues). Total 13 pages.

Table S1. Chemical shift data for assigned residues in *Nm*HO-DMDH-CN and *Nm*HO-PH-CN complexes[a]

		$\square_{DSS}$(obs)[a]				
		*Nm*HO'-DMDH-CN			*Nm*HO'-PH-CN[b]	$\square\square_{dip}$(calc)[c]
Residue	Proton	i=A[d]	i = X[e]	i = Z[f]	i = A	
Ala12	NH	9.00	9.03		8.96	0.07
	$C_{\square}H$	3.38	3.39		3.30	0.12
	$C_{\square}H_3$	1.09	1.10		1.02	0.1
Leu15	$C_{\square}H$	0.62			0.57	0.1
	$C_{\square 1}H_3$	-0.55			-0.65	0.12
	$C_{\square 2}H_3$	0.08			0.21	0.11
Ala17	NH	8.60	8.67		8.10	0.18
	$C_{\square}H$	4.45	4.50		4.35	0.15
	$C_{\square}H_3$	1.75	1.72		1.64	0.1
Asp18	NH	8.92	8.67		8.64	0.12
	$C_{\square}H$	5.01	5.03		4.97	0.07
	$C_{\square}H_3$	2.45	2.42	2.39	2.27	0.2
	$C_{\square 2}H$	2.89	2.91		2.85	0.09
Thr19	NH	8.16	8.27		8.04	0.17
	$C_{\square}H$	5.55	5.52		5.52	0.05
	$C_{\square}H$	5.83	5.80		5.75	0.08
	$O_{\square}H$	6.21	6.00		5.90	0.26
	$C_{\square}H_3$	1.72	1.75		1.70	0.08
Thr20	NH	8.52	8.61		8.37	0.18
	$C_{\square}H$	6.52	6.68	6.28	6.30	0.33
	$C_{\square}H$	5.30	5.32	5.19	5.14	0.15
	$C_{\square}H_3$	2.45	2.42	2.39	2.27	0.2
Ala21	NH	9.41	9.38		9.36	0.05
	$C_{\square}H$	5.23	5.30		5.31	-0.03
	$C_{\square}H_3$	1.96	2.00		2.04	-0.02
Val22	NH	9.36	9.22		9.44	-0.07
	$C_{\square}H$				4.87	-0.21
	$C_{\square}H$	2.50	2.58		2.72	-0.13
	$C_{\square 1}H_3$	1.30	1.32		1.50	-0.15
	$C_{\square 2}H_3$	1.18	1.19		1.40	-0.24
His23	NH	10.87	10.98		11.08	-0.19
	$C_{\square}H$	6.12	6.13	7.22	7.37	-1.2
	$C_{\square 1}H$	11.45	11.30	11.87	11.56	
	$C_{\square 2}H$	10.33	10.57	9.40	10.75	
Asp24	NH	11.29	11.26		11.41	-0.27
	$C_{\square}H$	6.37	6.42		6.80	-0.45
	$C_{\square 1}H$	3.43	3.60		3.65	-0.13

	$C_{\square 2}H$	4.14	4.17		4.30	-0.14
Ser25	NH	8.38	8.40		8.77	-0.35
Val26	NH	7.56	7.61		8.33	-0.68
	$C_{\square}H$	2.26	2.31	2.96	2.80	-0.48
	$C_{\square}H$	0.06	0.23	1.89	1.60	-1.56
	$C_{\square 1}H_3$	-3.28	-3.08	-1.91	-1.96	-0.98
	$C_{\square 2}H_3$	-0.30	-0.17	0.75	0.51	-0.67
Asp27	$C_{\square}H$	-0.40	-0.33			-0.15
	$C_{\square 1}H$	2.77	2.55			-0.34
	$C_{\square 2}H$	0.11	0.35			-0.7
Val30	NH	7.61	7.59		7.87	-0.12
	$C_{\square}H$	2.40	2.47		2.46	0.02
	$C_{\square}H$	0.25	0.38		0.40	0.13
	$C_{\square 1}H_3$	-0.71	-0.67		-0.68	0.27
	$C_{\square 2}H_3$	-0.14	-0.11	-1.03	-0.21	-0.02
Val33	NH	6.56	0.58		6.54	0.02
	$C_{\square}H$	4.06	4.07		4.05	0.02
	$C_{\square}H$	1.66	1.66		1.62	0.02
	$C_{\square 1}H_3$	0.28	0.28		0.29	-0.01
	$C_{\square 2}H_3$	-0.54	-0.51		-0.55	0.02
Phe36	$C_{\square}Hs$	6.91	6.99		6.80	0.12
	$C_{\square}Hs$	6.69	6.50		6.64	0.2
Tyr42	$C_{\square}Hs$	6.92	6.95		6.84	0.07
	$C_{\square}Hs$	6.98	6.95		6.79	0.09
	OH	9.23	9.28		9.16	0.09
Phe45	$C_{\square}Hs$	6.70	6.56		6.77	0.13
	$C_{\square}Hs$	7.19	7.10		7.23	0.24
	$C_{\square}H$	7.31	7.67		7.34	0.4
Gln49	$N_{\square 1}H$	10.78	10.70		10.14	0.08
	$N_{\square 2}H$	8.20	7.98		7.35	0.14
Phe52	$C_{\square}Hs$	6.69	6.56		6.55	-0.05
	$C_{\square}Hs$	6.60	6.58		6.71	-0.08
	$C_{\square}H$	6.04	6.08		6.41	-0.08
His53	$N_{\square 1}H$	12.01	11.89		12.13	0.09
Val81	$C_{\square}H$	3.76	3.75		3.62	0.04
	$C_{\square}H$	1.77	1.75		1.77	0.03
	$C_{\square 1}H_3$	0.74	0.74		0.63	0.04
	$C_{\square 2}H_3$	0.50	0.49		0.39	0.05
Trp110	$C_{\square 1}H$	7.22	7.20		7.27	-0.01
	$N_{\square 1}H$	11.44	11.47		11.52	-0.02
	$C_{\square 3}H$	6.92	6.94		6.95	-0.03
	$C_{\square 2}H$	7.19	7.20		7.27	-0.04

	$C_{\square 3}H$	6.45	6.47	6.48	-0.05
	$C_{\square 2}H$	6.30	6.30	6.38	-0.05
Cys113	NH	7.30		7.40	0.1
	$C_{\square}H$	2.59	2.64	2.60	0.23
	$C_{\square 1}H$	2.32	2.31	2.32	0
	$C_{\square 2}H$	2.09	2.07	2.04	0.02
Ala114	NH	7.86	7.92	8.04	0.04
	$C_{\square}H$	3.71	3.68	3.71	0.01
	$C_{\square 1}H_3$	1.54	1.49	1.60	0.01
Glu115	NH	8.95	8.96	9.07	0.07
	$C_{\square}H$	3.95	3.99	4.01	0.01
Gly116	NH	7.91	7.95	7.95	0.22
	$C_{\square 1}H$	0.33	0.50	0.55	0.66
	$C_{\square 2}H$	0.65	0.70	0.95	0.16
Ser117	NH	5.82	5.95	6.12	0.22
Asn118	NH	8.52		8.46	-0.13
Leu119	NH	8.23	8.60	10.54	-0.74
	$C_{\square}H$	3.84	3.85	4.72	-0.54
	$C_{\square 1}H$	-1.84	-2.24	-1.15	-0.63
	$C_{\square 2}H$	-1.74	-1.83	-0.95	-0.35
	$C_{\square}H$	-1.07	-0.96	-0.40	-0.93
	$C_{\square 1}H_3$	-1.67	-1.43	-1.69	-0.36
	$C_{\square 2}H_3$	-0.98	-0.96	-0.63	-0.25
Gly120	NH			13.60	-2.66
	$C_{\square 2}H$			5.75	-2.88
Ala121	NH	14.50	14.58	15.32	-0.98
	$C_{\square}H$	8.77	8.47	8.52	0.52
	$C_{\square}H_3$	4.90	4.90	5.44	0.04
Ala122	NH			9.73	-0.6
	$C_{\square}H$			4.93	-0.13
	$C_{\square}H_3$			1.98	-0.32
Phe123	NH	8.70	8.61	8.83	-0.09
	$C_{\square}H$	4.33	4.40	4.51	0.08
	$C_{\square 1}H$	3.22	3.30	3.46	0.51
	$C_{\square 2}H$	3.13	3.29	3.27	0.11
	$C_{\square}Hs$	6.97	7.09	7.07	0.32
	$C_{\square}Hs$	6.77	6.89	6.94	0.2
	$C_{\square}H$	7.28		7.15	0.15
Leu124	NH	8.53	8.63	8.09	0.54
Phe125	NH	10.52	10.39	10.00	0.18
	$C_{\square}H$	4.54	4.54	4.47	0.11
	$C_{\square}Hs$	7.48	7.47	7.50	0.02
	$C_{\square}Hs$	7.45	7.40	7.40	0.01

Lys126	NH	7.33	7.40	7.75	0.08
His127	C□H	6.30	6.43	6.21	0.08
	C□H	7.38	7.42	7.36	0.1
Tyr133	NH	6.97	6.89	6.97	0.04
	C□H	5.36	5.36	5.34	0.03
	C□1H	2.35	2.36	2.32	0.05
	C□2H	3.54	3.55	3.50	0.06
	C□Hs	6.66	6.68	6.64	0.05
	C□Hs	6.60	6.60	6.57	0.04
Asn134	NH	9.07	9.07	9.09	0.03
His137	NH	7.55	7.56	7.54	0.02
	C□H	4.93	4.92	4.92	0.02
	C□1H	3.09	3.09	3.05	0.02
	C□2H	3.29	3.29	3.25	0.02
	C□H	7.20	7.12	7.12	0.02
	C□H	8.00	8.06	8.00	0.01
Gly138	NH	10.43	10.43	10.43	0.02
	C□1H	3.90	3.91	3.87	0.04
	C□2H	3.56	3.71	3.54	0.04
Ala139	NH	7.88	7.88	7.82	0.03
	C□H	4.93	4.90	4.82	0.07
	C□H_3	1.42	1.40	1.36	0.06
Arg140	NH	12.46	12.47	12.33	0.04
	C□H	4.20	4.19	4.18	0.02
	C□1H	1.83	1.87	1.88	0.01
	C□2H	1.90	1.93	1.72	0.03
	N□H	10.06	10.02	9.93	0.01
	N□1H	6.74	6.72	6.74	0.01
	N□2H	6.98	7.00	6.96	0.01
His141	NH	11.12	11.03	10.91	0.05
	C□H	4.50	4.52	4.46	0.03
	C□1H	1.40	1.40	1.36	0.05
	C□2H	1.40	1.40	1.36	0.05
	C□2H	6.94	6.95	6.75	0.13
	C□1H	7.98	7.98	7.78	0.12
	N□1H	13.68	13.70	13.56	0.07
Leu142	NH	7.36	7.33	7.23	0.06
	C□H	5.45	5.42	5.30	0.08
His145	C□H	6.67	6.67	6.67	-0.04
	C□H	7.70	7.70	7.71	-0.03
Asp147	NH	10.95	10.97	11.04	-0.05
	C□H	4.69	4.70	4.77	-0.04
	C□1H	2.70	2.71	2.74	-0.04
	C□2H	2.91	2.91	2.94	-0.05

Trp153	$C_{\square1}H$	6.33	6.34	6.37	-0.07
	$N_{\square1}H$	8.83	8.97	8.69	0.07
	$C_{\square3}H$	6.98	7.01	7.09	-0.03
	$C_{\square2}H$	6.58	6.61	6.43	0.26
	$C_{\square3}H$	5.83	5.87	5.87	0.1
	$C_{\square2}H$	6.16	6.22	6.09	0.27
Phe156	$C_{\square}Hs$	6.74		6.75	0.03
	$C_{\square}Hs$	6.63		6.60	0.05
	$C_{\square}H$	6.85		6.89	0.05
Val157	NH	8.23	8.23	8.28	0.01
	$C_{\square}H$	2.61	2.62	2.65	0.05
	$C_{\square}H$	1.27	1.29	1.28	0.03
	$C_{\square1}H_3$	0.10	0.10	0.05	0.05
	$C_{\square2}H_3$	-0.48	-0.48	-0.42	0.06
Asn161	$N_{\square1}H$	7.22	7.23	7.22	0.05
	$N_{\square2}H$	6.17	6.18	6.16	0.07
Ala180	NH	8.18	8.20	8.28	-0.05
	$C_{\square}H$	2.24	2.26	2.28	-0.08
	$C_{\square}H_3$	0.04	0.07	0.26	-0.07
Phe181	NH	7.56		7.82	-0.14
	$C_{\square}Hs$	6.71	6.77	7.25	-0.48
	$C_{\square}Hs$	6.85	6.92	7.72	-0.91
	$C_{\square}H$	8.87	8.77	8.87	0.31
Phe183	$C_{\square}Hs$	7.10	7.10	7.11	-0.07
	$C_{\square}Hs$	7.24	7.27	7.36	-0.04
	$C_{\square}H$	6.72	6.71	6.77	-0.03
Tyr184	$C_{\square}Hs$	5.01	5.03	5.20	-0.24
	$C_{\square}Hs$	5.32	5.32	5.35	-0.11
	OH	7.92	7.80	7.44	0.1
Val186	NH	7.56	7.46	7.66	-0.11
	$C_{\square}H$	3.32	3.33	3.45	-0.07
	$C_{\square}H$	2.12	2.13	2.24	-0.07
	$C_{\square1}H_3$	1.00	1.01	1.10	-0.05
	$C_{\square2}H_3$	0.78	0.80	0.87	-0.07
Val187	NH	7.56	7.60	7.73	-0.08
	$C_{\square}H$	3.11	3.12	3.13	-0.04
	$C_{\square}H$	1.03	1.04	1.11	-0.07
	$C_{\square1}H_3$	0.39	0.39	0.45	-0.03
	$C_{\square2}H_3$	-0.22	-0.22	-0.18	-0.05
Phe192	$C_{\square}Hs$	7.27		7.32	
	$C_{\square}Hs$	6.75		6.74	
His207	NH	9.68		9.15	
	$C_{\square}H$	3.90		4.04	

	$C_{\beta}H$	1.90	2.22
	$C_{\beta}H'$	2.16	2.43
	$C_{\delta 2}H$	6.50	6.48
	$C_{\epsilon 1}H$	7.58	7.53
Arg208	NH	8.19	
	$C_{\alpha}H$		3.84

a) Chemical shifts in ppm, referenced to DSS via the residual solvent peak, in ^1H_2O, pH 7.0 at 25°C.

b) In ppm, referenced to DSS, in ^1H_2O, 100 mM phosphate, pH 7.0 at 25°C, as reported in Ref. (*31*).

c) Difference in calculated dipolar shift, $\Delta\delta_{dip}$(calc) = δ_{dip}(calc:*Nm*HO^A-DMDH-CN) - δ_{dip}(calc:*Nm*HO^A-PH-CN), on the basis of magnetic axes (α = 200°, β = 8°, γ = 40°) for *Nm*HO^A-PH-CN and (α = 215°, β = 12°, γ = 40°) for *Nm*HO^A-DMDH-CN, using the conserved $\Delta\chi_{ax}$ = 2.48 x 10^{-8} m^3/mol and $\Delta\chi_{rh}$ = -0.58 x 10^{-8} m^3/mol (*31, 60*)

d) The dominant complex in high phosphate concentration (100 mM), consisting of the Ser2-His209 polypeptide.

e) The "aged" complex, in 100 mM phosphate, consisting of the Ser2-His207 polypeptide.

f) The equilibrium isomeric form of the Ser2-His209 polypeptide stabilized at low phosphate concentration.

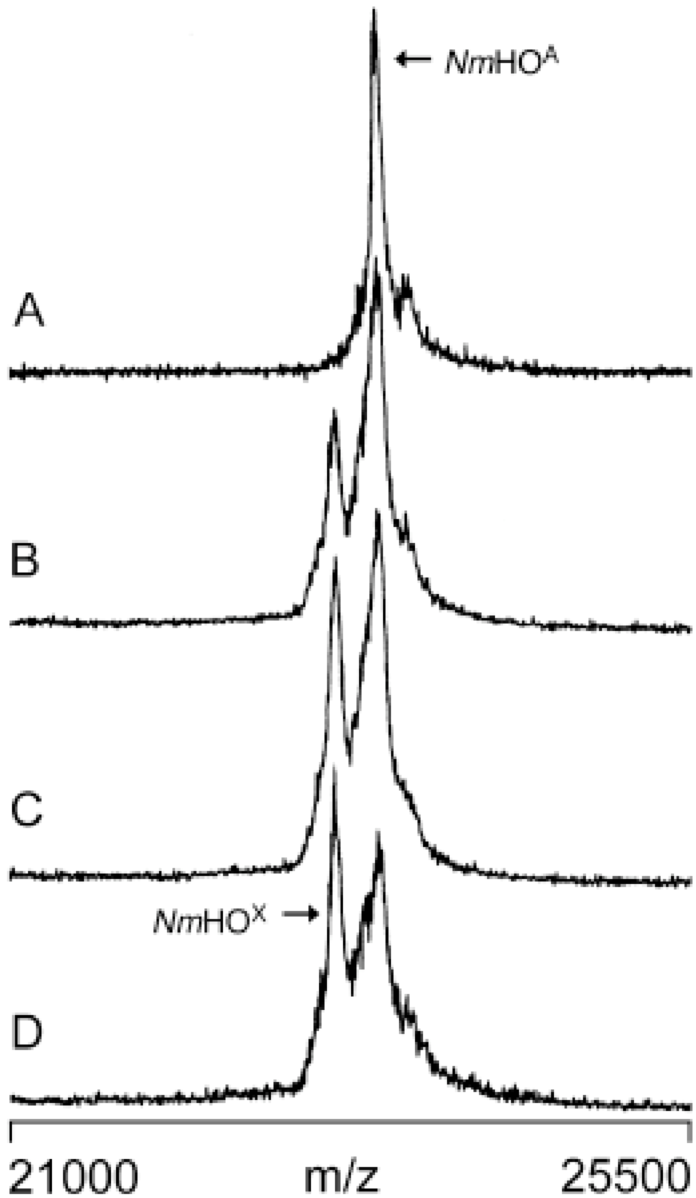

Figure S1. MALDI-TOF mass spectra of (**A**) >95% *Nm*HO^{A}-DMDH-CN; (**B**) ~80% *Nm*HO^{A}-DMDH-CN, ~20% *Nm*HO^{X}-DMDH-CN; (**C**) ~60% *Nm*HO^{A}-DMDH-CN, ~40% *Nm*HO^{X}-DMDH-CN; (**D**) ~50% *Nm*HO^{A}-DMDH-CN, ~50% *Nm*HO^{X}-DMDH-CN, with ^{1}H NMR spectrum as shown in Figure 2C.

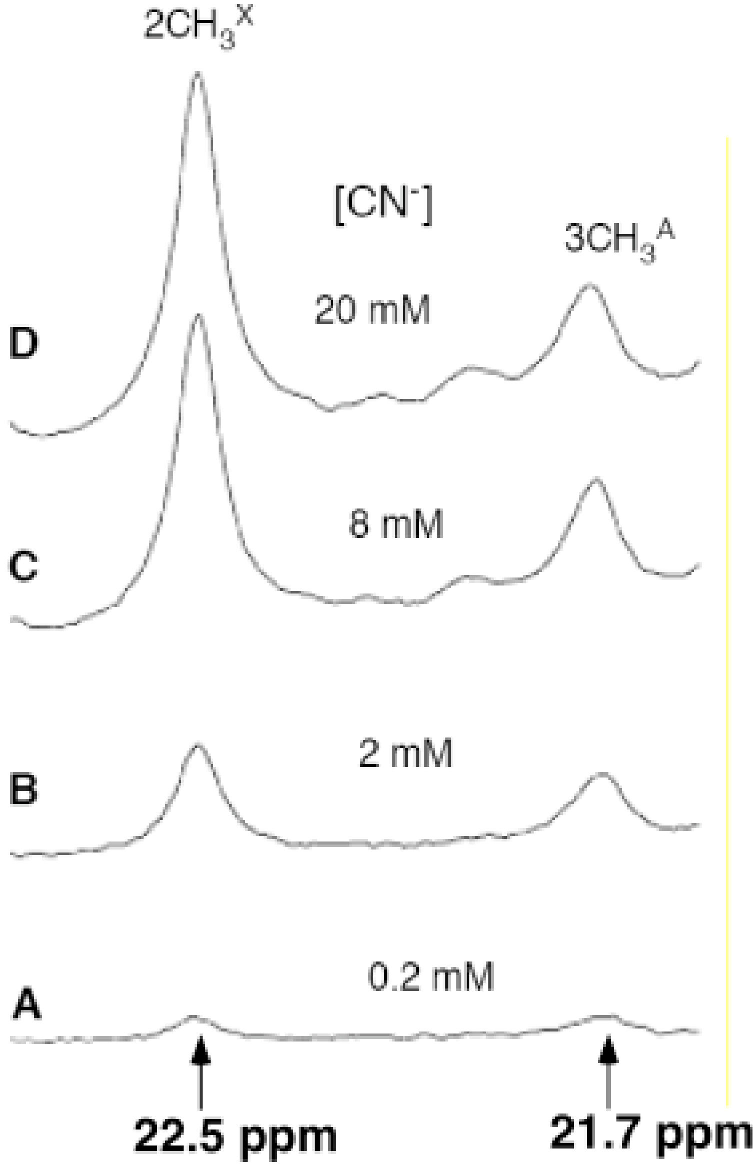

Figure S2. Low-field portion of the 600 MHz ^{1}H NMR spectra of the *Nm*HO-DMDH-CN complexes from a ~3:10 *Nm*HO^A-DMDH-H_2O:*Nm*HO^X-DMDH-H_2O mixture in ^1H_2O, 100 mM phosphate, pH 7.2 at 25°C, as a function of [KCN], in mM. The appearance of equal amounts of *Nm*HO^A-DMDH-CN and *Nm*HO^X-DMDH-CN at low [KCN] for the 3:10 'A':'X' mixture yields a ratio of equilibrium constant for CN^- binding of K_{eq}(*Nm*HO^A-DMDH-CN)/K_{eq}(*Nm*HO^X-DMDH-CN) ~3.3.

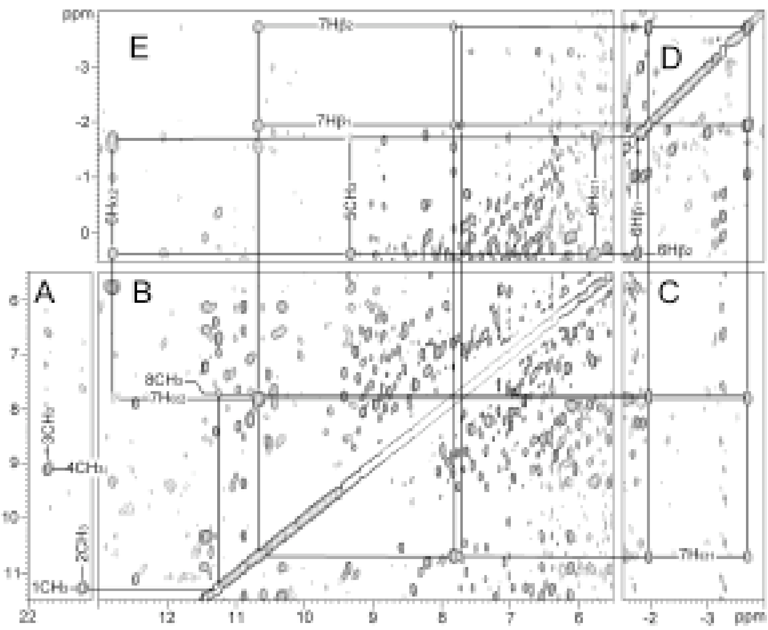

Figure S3. Portions of the 600 MHz ^{1}H NMR NOESY spectrum (mixing time 40 ms, repetition rate 2 s^{-1}) of *Nm*HO^{A}-DMDH-CN in $^{1}H_2O$, 100 mM in phosphate, pH 7.2 at 25°C, illustrating the contacts among DMDH pyrrole substituents. Starting with pyrrole A, shown are the $1CH_3$-$2CH_3$ (and $3CH_3$-$4CH_3$) (**A**), $1CH_3$ - $8CH_3$ (**B**), $8CH_3$ - 7-propionate (**B**, **C**), and 6-propionate - $5CH_3$ (**D**, **E**) contacts. The expected $2CH_3$ - $3CH_3$ cross peak is 0.5 ppm from the diagonal and is observed only in the slice (not shown); and the expected $4CH_3$ - $5CH_3$ cross peak is too close to the diagonal (0.15 ppm) to resolve.

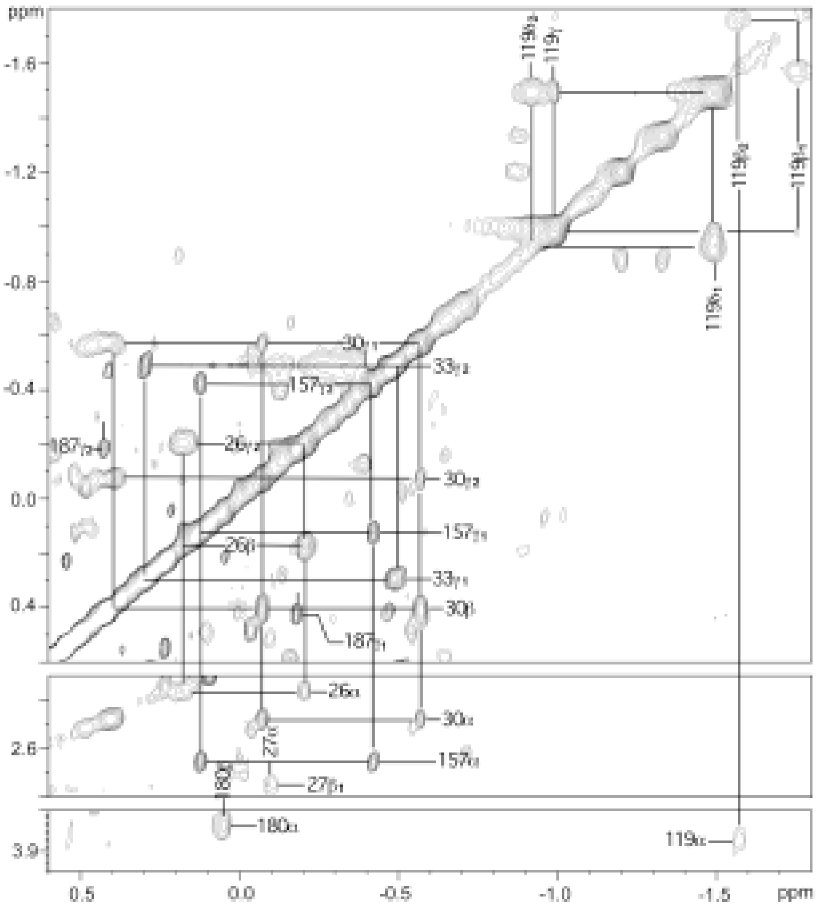

Figure S4. Portions of the 500 MHz ^{1}H NMR TOCSY spectrum (mixing time 29 ms, repetition rate 0.7 s^{-1}) of *Nm*HO^{A}-DMDH-CN in $^{1}H_2O$, 100 mM in phosphate, pH 7.2 at 25°C, illustrating the scalar connection for the upfield dipolar shifted Val26, Asp27, Val30, Val33, Leu119, Val157, Ala180 and Val187.

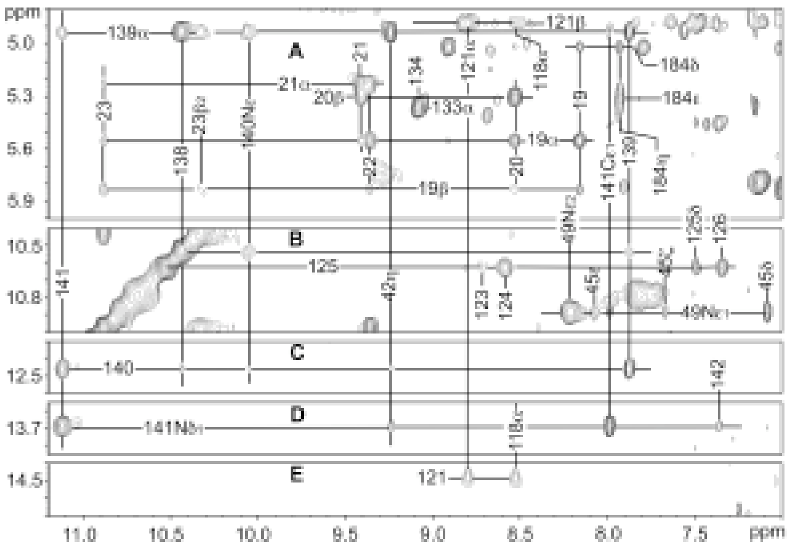

Figure S5. Portions of the 600 MHz ^{1}H NMR NOESY spectrum (mixing time 40 ms, repetition rate 1 s^{-1}) for *Nm*HO^{A}-DMDH-CN in $^{1}H_2O$, 100 mM in phosphate, pH 7.2 at 25°C, illustrating sequential contacts for the proximal helix residues Asp18-His23 (**A**), distal helix residues Asn118-Ala121 and Phe123-Lys126 (**A**, **B**, **E**), and loops Ala139-Leu142 (**A**, **C**), contacts between Gln49 and Phe45 (**B**) that confirm (*31, 36*) the 180° □-□rotation of the Gln side chain relative to the crystal (*15, 22*), and key contacts to the residues involved in strong H-bonds (**A**-**D**).

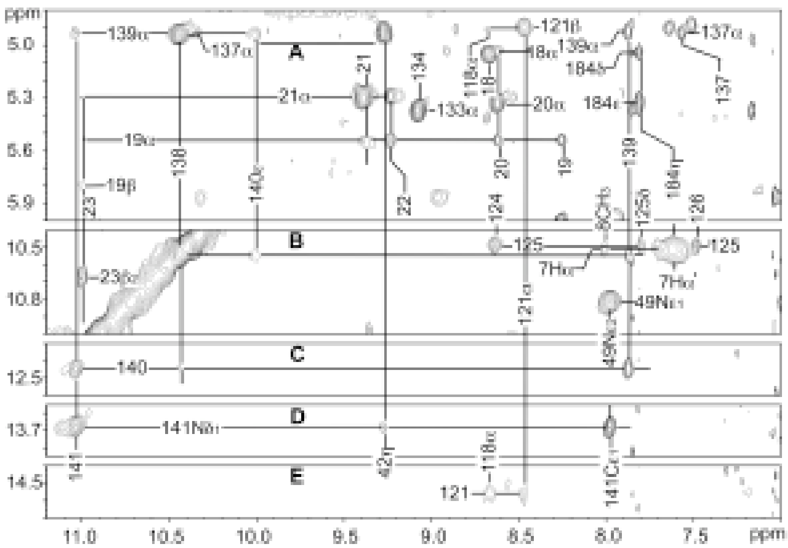

Figure S6. Portion of the 600 MHz ^{1}H NMR NOESY spectrum (mixing time 40 ms; repetition rate 1 s^{-1}) of *Nm*HO^{X}-DMDH-CN in $^{1}H_2O$, 100 mM phosphate, pH 7.2 at 25°C, illustrating essentially the same contacts for the 'X' complex of DMDH as described for the 'A' complex in Figure S5.

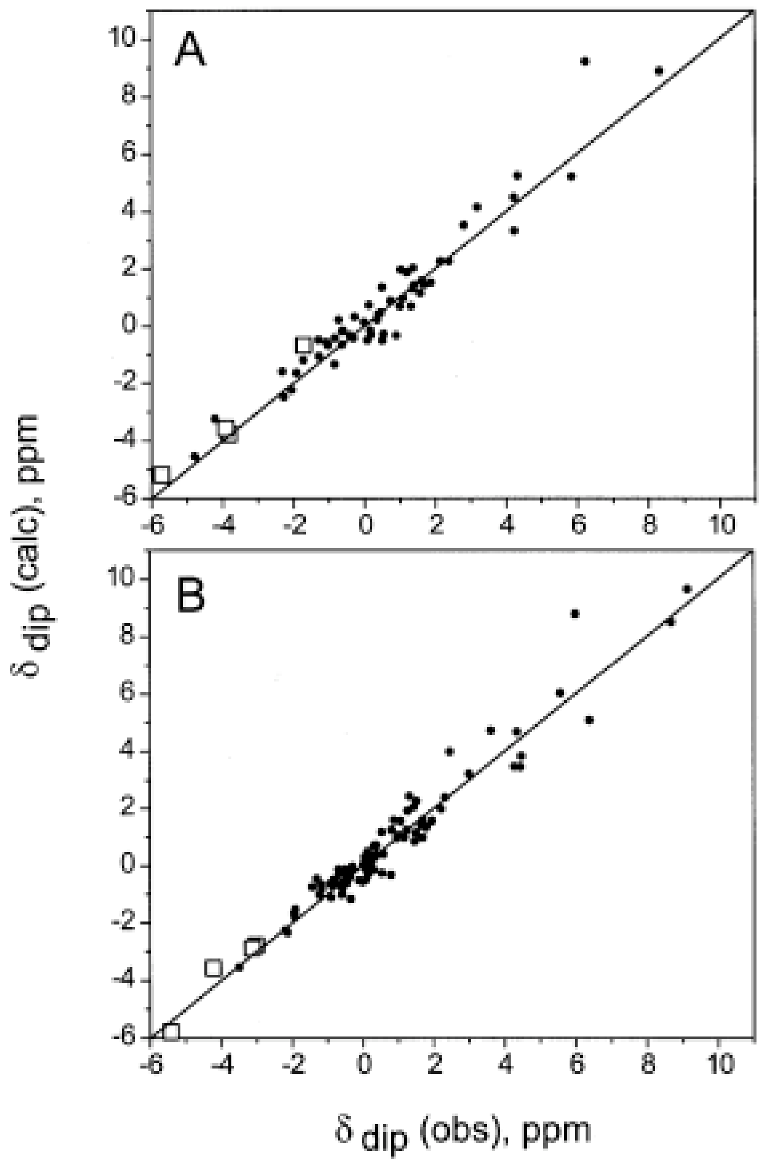

Figure S7. Plots of δ_{dip}(obs) versus δ_{dip}(calc) for the optimized magnetic axes of: (**A**) *Nm*HO[A]-DMDH-CN with $\Delta\chi_{ax}$ = 2.48 x 10^{-8} m^3/mol, $\Delta\chi_{rh}$ = -0.58 x 10^{-8} m^3/mol, α = 215 ± 10°, β = 12 ± 1° and κ = 40 ± 15°, and (**B**) *Nm*HO[A]-PH-CN with $\Delta\chi_{ax}$ = 2.48 x 10^{-8} m^3/mol, $\Delta\chi_{rh}$ = -0.58 x 10^{-8} m^3/mol, α = 200 ± 10°, β = 8 ± 1° and κ = 40 ± 10°, each determined from three parameter searches to obtain α, β and κ, using as input only δ_{dip}(obs) for residues assigned for both the DMDH and PH complexes, and retaining the strongly conserved anisotropies for His/CN^- ligated ferrihemoproteins reported previously. (*31, 60*) The data points correspond to input data (closed circles) and open squares (the heme propionate C□Hs).